

**ECMM102**

Group Project (Meng) (A, TRM1+2 2017/8)

**046433**

1029797

**Coursework:** Individual contribution to the group achievement**Submission Deadline:** Mon 14th May 2018 12:00**Personal tutor:** Professor Fayyaz Memon**Marker name:** Tabor

630029451

**Word count:** 8995

By submitting coursework you declare that you understand and consent to the University policies regarding plagiarism and mitigation (these can be seen online at [www.exeter.ac.uk/plagiarism](http://www.exeter.ac.uk/plagiarism), and [www.exeter.ac.uk/mitigation](http://www.exeter.ac.uk/mitigation) respectively), and that you have read your school's rules for submission of written coursework, for example rules on maximum and minimum number of words. Indicative/first marks are provisional only.

First marker's comments

Indicative mark

Second marker's comments

Second mark

Moderator's comments

Agreed mark





## I2 Report

The Use of the Drift Flux Model to Simulate  
a Hydrodynamic Vortex Separator in  
OpenFOAM<sup>®</sup>

**Thomas Russell**

2018

4<sup>th</sup> Year MEng Group Project

I certify that all material in this thesis that is not my own work has been identified and that no material has been included for which a degree has previously been conferred on me.

A handwritten signature in black ink, appearing to read "Thomas Russell".

Signed.....

College of Engineering, Mathematics, and Physical Sciences  
University of Exeter

# I2 Report

## ECMM102

Title: The Use of the Drift Flux Model to Simulate a Hydrodynamic Vortex Separator in OpenFOAM®

Word count: 8995

Number of pages: 40

Date of submission: 14/05/2018

Sudent Name: Thomas Russell

Programme: Mechanical Engineering MEng

Student Number: 630029451

Candidate Number: 011484

Supervisor: Dr. Gavin Tabor

## Abstract

The aim of this project was to implement a viable numerical scheme to accurately model a Hydrodynamic Vortex Separator (HDVS) using the open source CFD package OpenFOAM®. To achieve this, research into various methods of multi-phase modelling was undertaken, particularly the Drift Flux Model.

The affect of changing interpolation and integration schemes was assessed in preliminary computational efficiency studies, including a comparison of GAMG and PCG linear-solvers.

The subsequent model was then compared to related empirical study. Insufficient simulation time caused by numerous computational setbacks meant a steady-state solution was not reached. Consequently, few meaningful similarities were found and validation could not be fully confirmed. Velocity and separation characteristics suggest comparable results could be produced if time had permitted. Quality of the analytical model was agreed, but validation against physical experiment was not possible.

Discussion into project management and limitations conclude the report, with mention of individual contribution to a group investigation.

**Key words:** Multi-phase flow, Drift Flux Model, CFD, OpenFOAM®, Hydrodynamic Vortex Separator

# Contents

<b>1</b>	<b>Introduction and Background</b>	<b>1</b>
1.1	Objective . . . . .	1
1.2	Specific Background . . . . .	2
1.2.1	Case Apparatus . . . . .	2
1.2.2	Settling and Vorticity . . . . .	4
<b>2</b>	<b>Literature review</b>	<b>5</b>
<b>3</b>	<b>Theoretical background and analytical investigation</b>	<b>8</b>
3.1	Single-Phase Flow . . . . .	8
3.2	Multi-Phase Flow . . . . .	10
3.2.1	Eulerian and Lagrangian Methods . . . . .	10
3.2.2	Drift Flux Model . . . . .	13
3.3	CFD discretisation and solving methods . . . . .	16
3.4	Computational Efficiency Study on Rectangular Tank . . . . .	21
3.4.1	Initial Conditions . . . . .	21
3.4.2	Finite Volume Schemes . . . . .	22
3.4.3	Finite Volume Solution . . . . .	23
3.4.4	Outcome . . . . .	24
3.5	Settling Model Implementation . . . . .	27

3.6 Optimum Case Setup for Swirl-Flo® . . . . .	28
<b>4 Presentation of analytical results</b>	<b>30</b>
4.1 Tangential Velocity Profiles . . . . .	31
4.2 Volume fraction of Dispersed Phase . . . . .	34
<b>5 Discussion and Conclusions</b>	<b>35</b>
<b>6 Project management, consideration of sustainability and health and safety</b>	<b>37</b>
<b>7 Contribution to group functioning</b>	<b>38</b>
<b>8 References</b>	<b>39</b>

# 1 Introduction and Background

The quality and efficiency of waste water treatment is a subject matter of great importance in modern society. There exists a man-made water cycle, both acting as a small tangent to and in parallel with, the natural water cycle. Urban Drainage Systems (UDS) could be described as the discipline of managing the interaction of human water use and that of the environment; extraction and reintegration of water to and from the cycle [11]. Wastewater can be categorised into four general stages: preliminary, primary, secondary and tertiary; each being nearer to clean water than the last. Methods of treating each class of wastewater vary. Early stages can be physically filtered, removing larger agglomerations of debris, whilst latter stages are chemically treated. The focus of this project is the treatment of primary wastewater, fluid that has had large debris removed, but a dispersed phase of small solid particles remains.

Methods of treating primary wastewater consist mainly of manipulating the flow in a certain way, to allow the solid particles to settle into a layer of sediment, known as a sludge bed. The sludge bed is then removed and the by-product, primary sludge, is disposed of. Following sludge removal, the cleaner water passes into the secondary wastewater treatment process, which is beyond the scope of this project. To achieve settling of the solid particles, the wastewater is passed through either a stationary tank, structure or some form of apparatus. The geometry of this apparatus influences fluid flow, inducing separation. The means of separation depends on the apparatus; various techniques exist, yet settling under gravity is a common factor. It is understandable that the influence of gravity on the settling of suspended particles will take time. As such, investigation into the performance of primary settling tanks (ST) serves as inspiration for this project.

## 1.1 Objective

Modern developments of Computational Fluid Dynamics (CFD) sees classical empirical design methods supplemented and improved upon with mathematical and computational modelling techniques. In the context of primary settling tanks, optimisation of sludge removal involves changing geometry or adding features such as scrapers and hoppers.

Results from a laboratory environment cannot be fully validated, however, without the comparison of relatable data from an analytical source. Once a robust mathematical model has been fabricated and validated, optimisation studies can proceed in the computational domain. Any conclusions made can then be implemented *in situ*, improving reliability as well as reducing cost and waste. The aim of this report is to perform CFD simulations, with the use of the open source software OpenFOAM®, on a primary sedimentation tank model and to validate said model against related empirical study. With reference to the associated G2 report [3], this work package aims to achieve deliverables (vii) and (viii), addressing objectives (iii) and (iv). The first section of this report consists of an investigation into current literature on the subject of multiphase CFD modelling in wastewater systems. There follows a comprehensive summary of research into multiphase mathematical modelling techniques, with the aim to successfully implement the most appropriate CFD solver scheme into an accurate model. Next, fabrication of this model will be detailed, and studies into optimum running conditions and computational efficiency studies described. The final section will provide comparison between the computational results and experimental results from equivalent empirical study, in conjunction with other group members.

## 1.2 Specific Background

### 1.2.1 Case Apparatus

Two water treatment apparatus will be of subject in this report; an ARMFIELD W7 model rectangular settling tank (to be referred to as RT hereonin) and a Hydrodynamic Vortex Separator (HDVS), named Swirl-Flo®. The RT consists of a narrow, long, hollow rectangular tank, with a weir at either end. The sludge enters over the initial weir, allowing the fluid to flow at a low velocity across the linear length. At this point the majority of the sediment settles to the bottom of the tank forming a sludge bed. The relatively cleaner water to flow out over the second weir. Modifications were made to the original RT; a sloping base and hopper were 3D printed and inserted to encourage the formed sludge bed to exit through the underflow. Figure 1.1 shows a render of the RT, made from colourless perspex, with the modifications in place. The first weir has been

cut away, for legibility of internal geometry.



*Figure 1.1: CAD geometry render of RT,  
made in SolidWorks® retrieved from [23]*

The Swirl-Flo® is a hollow, cylindrical tank, that takes sludge in parallel with the internal wall. This angle of attack, higher inlet velocity and internal geometry, induces a swirling vortex of the subject fluid. Sediment in the fluid moves outwards, towards the internal walls, and upon interacting with the stationary boundary layer slows and drops to the bottom of the tank, exiting through an underflow. Clean water exits at an overflow at the top of the tank.

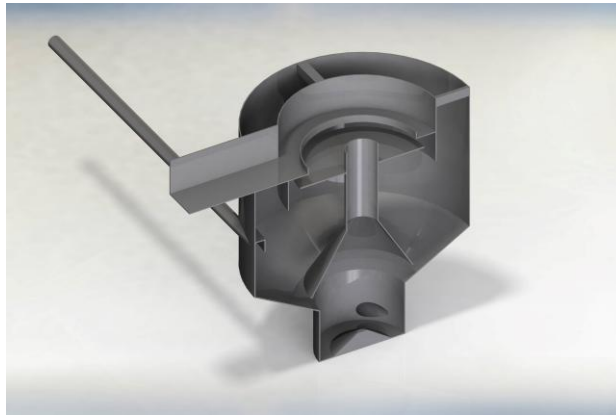


*Figure 1.2: Cross-section of Swirl-Flo® CAD Geometry,  
made in SolidWorks® retrieved from [23]*

The main difference between the two apparatus, from a modelling point of view, can be seen as the difference in the forces inducing particle settling. Settling occurs in the RT due only to gravity, the slow flow velocity gives sufficient time for the solid phase to fall

out of suspension. As well as gravity, centrifugal force due to vortex flow accelerates Swirl-Flo® sediment towards the boundary layer.

In this report, the RT CFD model will be mainly of use to test validity of the application solver to be selected, and be the subject of any computational efficiency studies. The findings from these will be carried on to perform accurate multiphase computational modelling, and true model validation of the Swirl-Flo®.

### 1.2.2 Settling and Vorticity

The above statement about the action of a fluid vortex is a large simplification; extensive research has gone into categorising and describing the behaviour of vortex fluid flow. Initially, a vortex can be formally described as “a swirling coherent structure in the flow that has time and length scales that are greater than the background scale of turbulence” [12]. They can be generally grouped into two types dependant on the characteristics of the vortex core: forced and free. A forced vortex is said to act in a similar manner to a ‘solid body’, where the viscous force of the fluid has a larger impact than any inertial force (represented by a low Reynolds number). This causes the tangential velocity to increase linearly with increasing radius:  $U_\theta = \Omega r$ , where  $U_\theta$  is the tangential velocity,  $\Omega$  is the angular velocity and  $r$  is the radius. In contrast, the inertial forces of a free vortex have a larger impact, and viscosity becomes negligible. This near-ideal, inviscid behaviour causes the angular momentum to remain constant:  $\rho A U_\theta * 2\pi r = k$ , where  $\rho$  is the fluid density and  $A$  is the flow area.

These behaviours are theoretical situations; real vorticity conforms to the Rankine vortex model [9]. A Rankine vortex can be simply characterised as having a forced vortex at the core, and a free vortex around the edges (tail) of the flow.

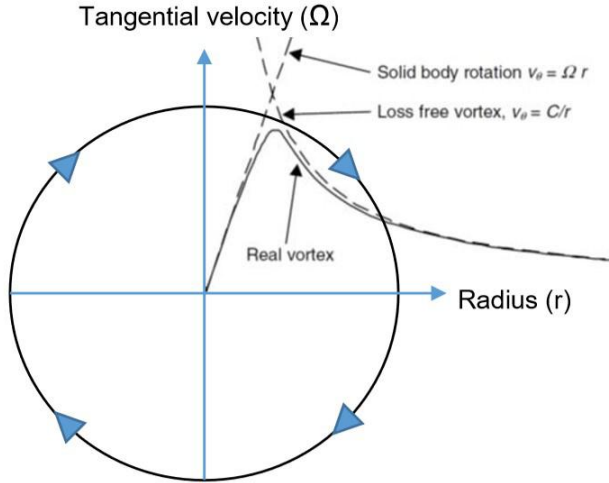


Figure 1.3: Real vortex behaviour, according to the Rankine vortex model, retrieved from [12]

This action is harnessed in the wastewater industry in primary settling tanks for a number of reasons. Vorticity of this kind can help minimise short-circuiting within the tank, increasing fluid residence time over a more traditional ST. This makes particle settling more likely and the capture rate higher. As previously mentioned, albeit briefly, the centrifugal force created by the vortex causes separation and settling. In contrast to a traditional ST, vorticity affects *particle* residence time and motion. As well as causing the particles to interact with the boundary layer, the swirling motion ‘sweeps’ the settled sediment towards the underflow at the centre bottom of the tank for extraction.

## 2 Literature review

Modelling a multiphase problem in the computational domain is a discipline of many approaches. Naturally the literature contains, almost exclusively, very specific scenarios. Nevertheless, critically analysing the methods and techniques gives some insight into completing this project objectives. There are numerous papers detailing the computational modelling of ST’s, findings of which will be carried onto the section of this report detailing computational efficiency studies. Fewer investigations detail the modelling of HDVS’s; the use of vorticity in the wastewater industry is a relatively new one, yet study of ST cases are still relevant due to similar mathematical techniques.

Larsen, 1977 [14] is the author of what can be seen as the earliest literature concerning

CFD modelling of a ST. Most other papers refer to parameters the author identified as influential to tank performance in their own work. The author's characterisation of fluid flow, and comparison to related numerical model, serves as the initial technique that the current literature relates to. Discussion of influential flow characteristics, such as recirculation or velocity and concentration distributions, serves as elaboration of previous ideal models into applicable findings.

Stamou and Rodi, 1989 [24] implemented the well known  $k - \epsilon$  turbulence model to ST's. This was with the aim to more realistically predict velocity and turbulent diffusivity distribution. Results compared well with associated experimental data.

The focus of accurately defining mixture properties was first detailed by Dahl, 1993 [7], to model secondary settling tanks (SST). Methods to find empirical values for settling parameters and other rheological findings were documented, employing a Bingham Plastic Model. These findings were implemented into the simulation. A dynamic similar to this will also be present in this report as communication with experimental results will be harnessed to more accurately model the scenario. Findings were scaled and compared with existing SST's in use. The author demonstrated the combination of an advanced numerical model and basic physical measurements to build a robust computational description.

A 3D computational model was fabricated by Liu and Garca 2011 [16], to simulate a primary ST similar to the model for preliminary study in this project. Attention was paid to the rheology of the fluid, akin to Dahl's work [7], a Bingham Plastic viscosity model was also used. This model reflected an ST that was then constructed.

Brennan, 2001 [5] described numerous methods of modelling multiphase flow, and related this to use of the Drift Flux Model in OpenFOAM®. Fabrication of a 3D model is then validated against experimental data.

Ahern, 2017 [1] presents a scenario and objectives very similar to this project, with respect to the use of OpenFOAM® to deliver a working CFD model for future optimisation. The study highlighted previously unknown flow field patterns in the subject ST. Similar to previous literature, the author applies the Drift Flux Model. This study could be improved upon, as also stated by the author, with comparison to empirical data.

A novel approach to ST modelling is documented in the work of Burt 2010 [6]. The author

suggests an extended Drift Flux Model, in which particles of various classes and settling characteristics can be modelled at once. A synthetic latex sludge is further suggested for use to replicate organic sludge in laboratory experiments. Implementation of various rheology models is a subject of mutual interest to the author and this project.

Jarman, 2011 [11] further details use of the Drift Flux Model to a flow case involving vorticity, a contrast to the numerous ST studies in the literature. The CFD models in this case was validated against laboratory data. There was note on the severe impact of turbulence modelling on the vortex flow, thus a heavy focus on turbulence theory. Application of multiphase modelling of vortex flow is of specific interest to this project, as the presence of investigations into modelling of HDVS is limited.

HDVS performance was also investigated in the computational domain, however, by Sansalone and Pathapati, 2009 [21]. Specifically a unit's response to unsteady rain runoff. This study exhibits use of a Lagrangian tracking approach for particles of varying size. Turbulence was also modelled, again the  $k - \epsilon$  model. The affect of a screen within a HDVS was tested by Schmitt *et al.*, 2013 [22]. A computational model, reflective of laboratory conditions, was fabricated with focus on both global and local CFD models. An Euler-Lagrangian approach was taken to track particles through the vortex.

Lee *et al.*, 2010 [15] predicted the particle removal efficiency of a HDVS in Fluent<sup>®</sup>. The authors defined standards for various parameters to help define performance and efficiency. These included particle size, surface loading rate and ratio of underflow to overflow. The velocity field was simulated using the RNG  $k - \epsilon$  model. Results were validated against empirical study.

Approaches and techniques studied in this review of the current literature will be taken forward to fulfil the objective of this report.

## **3 Theoretical background and analytical investigation**

This section introduces the theoretical and analytical techniques to be used in modelling the project scenario; from detailing the governing equations, how multiphase modelling relates to the CFD software and how this knowledge was applied to reaching the project objectives.

The research that follows becomes relevant with respect to how mathematical models of fluid flow are harnessed and expressed in CFD software.

The task of numerical solver selection is one of up-most importance; this will determine the accuracy of the computational model, and therefore the legitimacy of any validation conclusions made in comparison to the experimental data. Many analytical techniques exist that are better suited to describe specific flow cases. For a meaningful decision to be made one must first assess and gain knowledge of the equations governing the fluid flow.

The theory and investigation of this report can be broken into three acts. The first of which consists of research into multiphase modelling theory, followed by application of findings and knowledge to the setting up of case files for multiphase simulations in OpenFOAM®. Further description of various studies into optimising the performance of RT simulation models will follow, and manipulation of how the solver runs to produce the most accurate and efficient computational model possible. An optimum HDVS case will then be written, collating the findings. This case will be the output, deliverable and objective of this report, once validated against experimental data.

### **3.1 Single-Phase Flow**

Assessment of various fluid modelling techniques starts with single-phase flow, by means of the Reynolds Averaged Navier-Stokes equations. Describing the general physics of the flow, they can exist in various forms. The most sensible for application here is in the form of a transport equation; one equation representing conservation of mass and one as

a conservation of momentum:

$$\frac{\delta \rho}{\delta t} + \nabla \cdot (\rho U) = M \quad (1)$$

$$\frac{\delta(\rho U)}{\delta t} + \nabla \cdot (\rho U U) = \nabla \cdot \sigma + f \quad (2)$$

Where  $\rho$  is density of the fluid,  $t$  is time,  $\nabla \cdot$  is the divergence term,  $U$  is the velocity of the fluid,  $M$  is the overall mass flux sources,  $\sigma$  is the fluid stress and  $f$  is external body forces.

Within the scope of this project, it is acceptable to assume the fluid to be incompressible, meaning the continuity equation can be reduced to  $\nabla \cdot U = 0$ . The spacial and temporal gradients, for a single-phase, isotropic, incompressible fluid, with no external mass sources or sinks, are therefore zero [11]. Thus, Navier-Stokes can be simplified to:

$$\nabla \cdot U = 0 \quad (3)$$

$$\rho \left( \frac{\delta U}{\delta t} + U \nabla \cdot U \right) = \nabla \cdot \sigma + f \quad (4)$$

Where the continuity equation now representing conservation of volume rather than mass, due to the incompressible nature of the flow. This form now consists of three transport equations (each Cartesian dimension) and four unknowns:  $u_x$ ,  $u_y$ ,  $u_z$  and pressure. This is solved through the continuity equation, causing for strong coupling and linearity, allowing a composite solution.

In the context of the finite volume method, the spacial domain is split into many small cells (a mesh), the equations of motion are integrated over the volume of each cell. Difference equations are then produced by application of divergence theorem, leaving the role of the solver scheme to then invert the subsequent matrices, harnessing a meaningful result (further discussed in section 3.3). This means not only must a fitting mathematical technique be selected to describe flow, but also in relation to mesh properties.

## 3.2 Multi-Phase Flow

For a more accurate relation to the physicality of experimental data, a multiphase model must be considered. The mathematical description of multiphase flow can be approached in a number of ways, starting from the categorisation of multiphase fluids. This is dependant mostly upon the topology of the phase interfaces, and the physical state of each phase (gas-liquid, liquid-solid and gas-solid) [10]. The variety in characteristics of multiphase fluids has given rise to numerous methods of mathematically modelling said fluid, with each case being better suited for a different application. Choosing the most appropriate model, therefore, should involve studying the over-arching methods of multiphase modelling.

### 3.2.1 Eulerian and Lagrangian Methods

In fluid mechanics, there exist different formulation frames of reference for describing fluid flow. An Eulerian method can be seen as a ‘field’ approach; physical quantities associated with the flow are solved at every point in a time-space field. In contrast to this, Lagrangian methodology could be seen as the ‘particle’ approach; the trajectories of individual fluid particles are calculated by the sum of body forces acting upon them. Two-phase flow can be seen to fit into one of three combinations of these principle frameworks: Euler-Lagrange, Euler-Euler and mixture approaches (see section 3.2.2) [1]

With an Euler-Lagrange method, the trajectory of each dispersed phase particle is tracked through the continuous phase, which is treated as an Eulerian field. The equation of motion of each particle, in it’s simplest form, describes the motion of the particle through the continuous phase, relating the local acceleration to the sum of forces acting upon it at each point of its trajectory [5]:

$$\rho \frac{\delta u_d}{\delta t} = \Sigma F \quad (5)$$

Where  $u_d$  is the velocity of the dispersed phase particle,  $\rho$  is the density and  $F$  is the individual external body force on said particle. Equation 5 shows how the motion of each particle depends heavily upon the external forces acting on them. Although possibly

increasing accuracy of the model, this greatly increases the computational cost of the method. This is due to the method of coupling the Lagrangian particles and Eulerian field. In this context, energy and momentum is transferred within inter-phase and inter-particle collisions; known as four-way coupling, or granular flow [8]. The  $F$  term can represent many forces and interactions, this causes the computational cost to increase exponentially with volume fraction of the dispersed phase; the more particles there are, the more interactions there will be. Simplified coupling parameters (one-way and two-way) are possible for fluids of varying dispersed phase volume fraction, nonetheless, mathematical models that use an Eulerian-Lagrange approach are rarely used in CFD, unless the fluid is extremely dilute ( $\alpha_d < 10^{-6}$ ). Due to the computational inefficiency, an Euler-Lagrange model shall not be considered for use in this project.

Euler-Euler formulations are more common, as the phases are treated as inter-penetrating continua. The Navier-Stokes equations describe flow of a single phase, within an Eulerian frame of reference, therefore an Euler-Euler model for multiphase flow can be viewed as solving the Navier-Stokes equations twice, for each phase. Phase coupling is achieved through defining sources and sinks within exchange terms of the conservation equations. Considering the transport of mass and momentum separately for each phase can be seen in the Two Fluids Model, as follows.

### 3.2.1.1 Two Fluids Model

The Two-fluids model consists of modified Navier-Stokes, eq.1, with an extra momentum transfer term at the end. No interphase mass transfer is considered. Conservation of mass and momentum of the two phases are defined in the continuity equation:

$$\alpha_1 + \alpha_2 = 1 \quad (6)$$

Followed by the transport of mass and momentum for each separate phase:

$$\frac{\delta(\alpha_1\rho_1)}{\delta t} + \nabla \cdot (\alpha_1\rho_1 U_1) = 0 \quad (7a)$$

$$\frac{\delta(\alpha_2\rho_2)}{\delta t} + \nabla \cdot (\alpha_2\rho_2 U_2) = 0 \quad (7b)$$

$$\frac{\delta(\alpha_1\rho_1 U_1)}{\delta t} + \nabla \cdot (\alpha_1\rho_1 U_1 U_1) = -\nabla p + \nabla \cdot (\mu_1 \nabla \alpha_1 U_1) + \alpha_1 f + \mathbb{I}_2 \quad (7c)$$

$$\frac{\delta(\alpha_2\rho_2 U_2)}{\delta t} + \nabla \cdot (\alpha_2\rho_2 U_2 U_2) = -\nabla p + \nabla \cdot (\mu_2 \nabla \alpha_2 U_2) + \alpha_2 f + \mathbb{I}_1 \quad (7d)$$

Where the terms  $\mathbb{I}_1$  and  $\mathbb{I}_2$  represent the momentum transfer between the two phases, by such phenomena as drag, lift or buoyancy [11].

However, modelling the inter-facial momentum transfer, represented by these terms, is precisely the source of some difficulties. Modelling two phases in this manner can create some numerical instability. For the Two-fluids model to be viable there must be numerous quantitative physical characteristics available for the model; such as the sludge rheology, the shape of sludge flocs and how they deform in high velocity gradients. This information is not readily available for sludge [10].

This method of modelling can produce a detailed, accurate result. Yet, it has been argued that the Two-fluids model could be too computationally expensive for scenarios similar to this project, [1, 5]. In order to improve efficiency, it is often assumed one way coupling is of sufficient description; dependant on the concentration of dispersed phase. This is due to the slip (or drift, as it shall be further referred to) between each phase being mainly due to gravity. This is especially true for settling tanks, there is a component of tangential velocity when concerning the Swirl-Flo®, due to centrifugal force, as mentioned in section 1.2.1. Furthermore, the main influences on this topic's flow are the mixture's rheology, buoyancy and settling velocity of the dispersed phase, all easily attainable through empirical study. With these assumptions, the terms of inter-phase momentum transfer,  $\mathbb{I}_i$ , can be equated to zero; omitting many mathematical considerations and reducing any possible problems of numerical instability. With these simplifications of the Two-fluids model, resolving two continuity and two momentum equations becomes unnecessary and inefficient. Treating the two phases as a mixture can be seen as a logical simplification of the Two-fluids model, homogenising the contribution of momentum from each phase into a single velocity field. Thus, the Mixture Model, also

known as the Drift Flux Model, was derived.

### 3.2.2 Drift Flux Model

Also known as the Mixture or Homogeneous Model, the Drift Flux Equations treat the two phases (dispersed and continuous) as a mixture; assuming one phase moves relative to the other at a constant drift velocity, like solid particles settling out of water under gravity. This improves upon the Two-Fluids model from an efficiency point of view, as there exist only three equations to be solved as opposed to four. For a full derivation of the Drift Flux Equations, the reader is referred to Kallio, 1996 [13]. In the interest of brevity, what follows is a brief mathematical route from the above Euler-Euler Two-Fluids model to the Drift Flux Equations in the form used by Brennan, 2001 [5].

As mentioned in the previous section, the momentum transferred from one phase is gained by the other; eliminating said terms when the momentum equations are summed, due to their equal and opposite nature. The lack of inter-phase momentum transfer means the continuity relationship can be described by the following:

$$\frac{\delta \rho_m}{\delta t} + \nabla \cdot (\rho_m \nu_m) = 0 \quad (8)$$

Where the subscript  $m$  denotes a property of the mixture. Derived from the continuity equation of the dispersed phase, equation 7, the Diffusion equation can be written as:

$$\frac{\delta \alpha_2 \rho_2}{\delta t} + \nabla \cdot (\alpha_2 \rho_2 \nu_m) = -\nabla \cdot (\alpha_2 \rho_2 \nu_{2m}) \quad (9)$$

And following the derivation from Kallio, 1996, the Mixture Momentum is:

$$\frac{\delta \rho_m \nu_m}{\delta t} + \nabla \cdot (\rho_m \nu_m \nu_m) = -\nabla \cdot P_m + \nabla \cdot [\tau + \tau^t - \sum \alpha_k \rho_k \nu_{km} \nu_{km}] + \rho_m g + M_m \quad (10)$$

Where  $M_m$  is the capillary force. In reference to modelling, this term can represent a momentum source or sink as it takes affect of surface tension. The RHS contains three tensor fluxes:

The viscous stress:

$$\tau = \sum \alpha_k \tau_k \quad (11)$$

The turbulent stress:

$$\tau^t = \sum \alpha_k \rho_k \nu'_k \nu'_k \quad (12)$$

And the diffusion stress:

$$\sum \alpha_k \rho_k \nu_{km} \nu_{km} \quad (13)$$

This diffusion stress term is of specific interest. It calculates the way the relative motion of the phases ‘diffuse’ the momentum, and has important influence on equation 9. It is worth noting at this point the mixture continuity and momentum equations (8 and 10) are akin to their single-phase counterparts apart from, mainly, the final two terms of the mixture momentum, related to settling.

Following on from this, to account for the turbulent diffusion of the dispersed phase, Brennan, 2001 [5] applies the Boussinesq hypothesis “in which the turbulent diffusion of a scalar property is modelled with the molecular diffusion”. Therefore:

$$-\rho u' \phi' = \rho \Gamma \nabla \phi \quad (14)$$

Where  $\Gamma$  is the turbulent diffusion coefficient. This is made equal to the eddy diffusivity [24].

Treating the relative phase velocity as  $\nu_r = \nu_1 - \nu_2$ , the volumetric flux for each phase can be defined as:

$$j_k = \alpha_k \nu_k \quad (15)$$

Therefore, the total volumetric flux is obviously:

$$j = \sum \alpha_k \nu_k \quad (16)$$

At this point it should be noted that the mixture velocity,  $\nu_m$ , is different from the term  $j$  defined above. This is due to the differing phase densities.

It is useful for the terms denoting drift velocity to be written in the form:

$$\nu_{1j} = -\alpha_2 \nu_r \quad (17a)$$

$$\nu_{2j} = \alpha_1 \nu_r \quad (17b)$$

This is in order to relate the diffusion velocity,  $\nu_{km}$  and drift velocities  $\nu_{kj}$  in the form:

$$\nu_{2m} = \frac{\rho_1}{\rho_m} \nu_{2j} = -\frac{\alpha_1}{\alpha_2} \frac{\rho_1}{\rho_m} \nu_{1j} \quad (18)$$

Key terms of interest are now succinctly defined. The final model is therefore:

Mixture Continuity Equation:

$$\frac{\delta \rho_m}{\delta t} + \nabla \cdot (\rho_m \nu_m) = 0 \quad (19)$$

Mixture Momentum Equation:

$$\frac{\delta \rho_m \nu_m}{\delta t} + \nabla \cdot (\rho_m \nu_m \nu_m) = -\nabla \cdot P_m + \nabla \cdot [\tau + \tau^t] - \nabla \cdot \left( \frac{\alpha_d}{1 - \alpha_d} \frac{\rho_c \rho_d}{\rho_m} \nu_{dj} \nu_{dj} \right) + \rho_m g + M_m \quad (20)$$

Dispersed Phase Continuity (Diffusion) Equation:

$$\frac{\delta \alpha_d}{\delta t} + \nabla \cdot (\alpha_d \nu_m) = -\nabla \cdot \left( \frac{\alpha_d \rho_c}{\rho_m} \nu_{dj} \right) + \nabla \cdot \Gamma \nabla \alpha_d \quad (21)$$

Subscript  $c$  and  $d$  denote the continuous and dispersed phases, respectively. Important terms to note include the volume fraction of the dispersed phase,  $\alpha_d$ , to measure the

performance of the sedimentation devices. Also the related drift velocity,  $\nu_{dj}$ , to be found through empirical study. Investigating the settling velocity will be of use to relate computational model to experimental conditions. Summarising the stress terms (equations 11-13), the Diffusion equation accounts for motion of the dispersed phase, relative to the mixture centre of mass. As discussed; rather than detailing the coupling of the phase, as per the Two-fluids model, Drift Flux is further simplified by a constitutive relationship where relative motion of the dispersed phase is assumed to be constant. This is a fundamental assumption of this mixture model; implying all particles of the dispersed phase are of the same mass and topology. It is possible, in other formulations, to extend the Drift Flux Model to model multiple densities, size classes and drift velocities of dispersed phase [6]. Use of this, so called, extended model is beyond the scope of this project.

Use of this mixture model, simplified relative to other multiphase models, does not come without drawbacks. The use of a single continuity equation does limit the resolution of relative phase motion, losing detail of the flow. This is seen as an acceptable compromise in the context of this report, however. The balance between improved computational efficiency, and description of both phases is seen as the main draw of the Drift Flux Model. This, and the ability to implement rheological properties from empirical study, are the main reasons why the Drift Flux Model was chosen for use in modelling this project scenario.

### 3.3 CFD discretisation and solving methods

With the multiphase mathematical model now selected, the way in which OpenFOAM<sup>®</sup> expresses its behaviour must be analysed. This in order to allow proper manipulation within the programme, to produce a stable and accurate simulation.

The application solver `driftFluxFoam` is for two incompressible fluids, applying the aforementioned mixture approach, with the Drift Flux approximation for relative motion of the phases [20]. The equation discretisation process is the way OpenFOAM<sup>®</sup>, and other CFD software for that matter, converts the above partial-differential equations (PDEs) into algebraic equations that can be solved for every cell in the domain. These parameters, the way they're solved and their interpolation schemes are all controlled from the

OpenFOAM® system directory, in `fvSchemes`. Terms worthy of note in `driftFluxFoam`, are diffusive and convective terms (in the momentum equations).

The diffusive term refers to the Laplace operator  $\nabla^2$ . For a more thorough method, the reader is referred to [1]. Simply, this term is integrated over the control volume and linearised to produce the expression [19]:

$$\int_V \nabla \bullet (\Gamma \nabla \phi) dV = \int_S d\mathbf{S} \bullet (\Gamma \nabla \phi) = \sum_f \Gamma_f \mathbf{S}_f \bullet (\nabla \phi)_f \quad (22)$$

It is at this point the relationship between mesh and solver shows its importance. If the neighbouring cells are orthogonal in nature the face gradient discretisation can be solved implicitly by the solver, using a matrix of unknown values (to be discussed). Non-orthogonality, however, results in the introduction of an additional explicit term that must be solved by interpolating cell centre gradients, increasing CPU time and lowering stability.

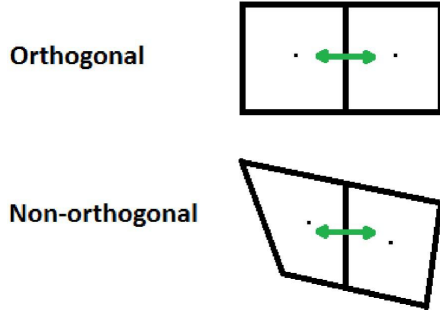


*Figure 3.1: Illustration representing orthogonality of neighbouring cells, retrieved from [19]*

The settings for this scheme can be adjusted in `fvSchemes`. This changes the interpolation scheme for each type of term. The general setting, from OpenFOAM®'s case tutorials, consists of:

```
laplacianSchemes
{
    default      Gauss linear corrected;
}
```

Meaning Gauss integration is to be applied, and the linear interpolation scheme; second order and above shall be used. Naturally, `default` means the same setting for all Laplacian terms shall be used. Various gradient schemes include:

```
Gauss linear orthogonal;
Gauss linear corrected;
Gauss linear uncorrected;
```

To take account of the mesh orthogonality characteristics.

Another term's discretisation worth mentioning is the convective term, relating to the divergence operator  $\nabla \bullet$ . The Drift Flux Model concerns the divergence of numerous values (see equations 20-21), so control of these schemes in `driftFluxFoam` is of importance. Similar to the integration and linearisation seen in 22, for the convection term:

$$\int_V \nabla \bullet (\rho \mathbf{U} \phi) dV = \int_S d\mathbf{S} \bullet (\rho \mathbf{U} \phi) = \sum_f \mathbf{S}_f \bullet (\rho \mathbf{U})_f \phi_f = \sum_f F \phi_f \quad (23)$$

Where  $\phi_f$  is the face field. The relation to the advection terms (volumetric flux on cell faces) means there are more differencing and integration schemes available. Each advection term behaves differently, so defining a `default` parameter would be nonsensical. The following is an example of how a different multiphase application solver, `interFoam`, is expressed in `fvSchemes` in the following manner:

```
divSchemes
{
    default           none;
    div(rhoPhi,U)    Gauss linearUpwind grad(U);
    div(phi,alpha)   Gauss vanLeer;
    div(phirb,alpha) Gauss linear;
    div(phi,k)       Gauss upwind;
    div(phi,epsilon) Gauss upwind;
    div((muEff*dev(T(grad(U))))) Gauss linear;
}
```

Where each term involving `div(phi, ...)` relates to the volumetric flux of the term on cell face  $\phi_f$ .

Adjustment of the interpolation scheme at this point will have an affect on the accuracy, stability and run time of the simulation.

The various interpolation schemes above include Upwind differencing (denoted by `upwind`), a first order bounded scheme, where  $\phi_f$  is determined from the direction of flow. This is considered inaccurate. An attempt to rectify this is with the option `linearUpwind`, a second order correction to Upwind differencing known as Blended differencing. Central differencing, `linear` interpolation, is second-order accurate but unbounded. Finally `vanLeer` implements Van Leer limited Central differencing [19, 25].

The computational evaluation of the above derivatives and differencing schemes can be done in an implicit or explicit manner. When performed implicitly, a matrix equation is created, of the form:

$$[M][x] = [q] \quad (24)$$

Where  $[M]$  is a matrix holding the unknown values, or more precisely, coefficients that correlate values between cell centres. The lower case  $[x]$  represents a column vector, holding values at the cell centres for which the linear system is to be solved, and  $[q]$  keeps source terms for each cell [25]. To find a solution, this linear set of equations must be evaluated. Inverting this matrix is the main cause for calculation time in simulations, and therefore appropriate manipulation can improve running efficiency. The parameters to control the linear system solver reside in `fvSolutions`.

Solver parameters and tolerances can be defined for each term. Another example from `interFoam`, for the term concerning volume phase fraction, `alpha.water` :

```
"alpha.water.*"
{
    nAlphaCorr      2;
    nAlphaSubCycles 1;
    cAlpha          1;
```

```

MULESCorr      yes;
nLimiterIter   3;

solver          smoothSolver;
smoother        symGaussSeidel;
tolerance       1e-8;
relTol          0;
}

```

This block contains information about the type of linear-solver to be used, smoothers and tolerances regarding iterations. The solvers are generally iterative, meaning they work by reducing the equation residual (error) over successive solutions. An equation is deemed sufficiently accurate once the residual falls below a certain tolerance, defined in `fvSolutions`. In the subject of the above example, when the residual for `alpha.water` drops below  $1 \times 10^{-8}$ , the solution will move to the next iteration. The parameter `relTol` is set to zero, due to the example being a transient case. Equations are often solved multiple times, however. Outer iterations usually represents an entire timestep or entire sweep of the transport equations, whilst the matrix solver iterations concern the number of times a specific equation is solved. Balancing the tolerance and number of iterations is key to producing an efficient simulation run that shall converge to an accurate solution. Each equation block will produce a matrix of slightly different characteristics, however. Symmetrical, asymmetrical or sparse all require different treatment for the quickest, most stable inversion. Advection terms (as are ever prevalent in `driftFluxFoam`) produce an asymmetric matrix, so only certain inversion methods can be used for these terms. Considered as the most common, or even first, are the Preconditioned Conjugate Gradient (PCG) and Geometric-Algebraic Multi-Grid (GAMG) solvers.

GAMG works by reaching a solution estimation on a coarse mesh, then mapping this approximation to the finer mesh supplied by the user. PCG, on the other hand, evaluates a descent method from the initial guess to the minimum, i.e. the solution. The steepest route cannot be used for a pathological case; re-establishing the path for every calculation or iteration for a highly elliptical parameter (as with the pressure field) would result in

an incredibly long path towards the minimum. PCG re-evaluates the steepest route as two axis, in conjugate directions, minimising the route in direction  $x_2$  and then  $x_1$ . This greatly reduces the decent method and therefore number of iterations, improving the efficiency for pathological cases.

The literature generally suggests GAMG for speed and PCG for accuracy [19]. This is, of course, dependant on a number of factors. GAMG is viable when the speed of initial solving on a coarse mesh outweighs the refinement and remapping process. Although asymmetric variants exist, PCG is only applicable to symmetrical cases and is especially good for highly elliptical, pathological cases.

Every conservation law for every outer iteration will produce matrices in the form of eq. 24; their solution can account for near 75% of CPU time [19] and the intrinsic reason why CFD is so computationally expensive. In the context of `driftFluxFoam`, there will be a heavy dependence on the solution of the pressure field - continuity equation 19. For these reasons, an efficient solution to the above issues in the pressure field is the focus of the following investigation.

## 3.4 Computational Efficiency Study on Rectangular Tank

### 3.4.1 Initial Conditions

The case files for an OpenFOAM® simulation of the RT were fabricated. A full investigation into this model was performed by an associate group member of the author, Bentley [4], the reader is referred to this work for detail.

A mesh of 629,466 cells was produced by the meshing portion of the group. In the interest of computational efficiency, the geometry of the tank was split down a symmetry plane. This is a common technique in the CFD community, literally halving the number of cells to be solved. For further detail the reader is referred to [23]. Initial conditions for the RT had to be imposed, to accurately represent physical behaviour of the equivalent laboratory model. For this laminar case of `driftFluxFoam`, the parameters that require description are the velocity `U`, dispersed phase `alpha.sludge` and pressure `p_rgh`. This term differs from the regular pressure field, as it neglects hydrostatic pressure. The Boundary conditions applied to each field are shown below, in table 3.1.

Table 3.1: Initial Conditions for the Rectangular Tank

Parameter	Inlet	Overflow	Underflow	Wall	Atmosphere	Symmetry
U	fixedValue	pressureInletOutletVelocity	fixedValue	fixed Value	slip	symmetryPlane
alpha.sludge	fixedValue	inletOutlet	zeroGradient	zeroGradient	slip	symmetryPlane
p_rgh	fixedFluxPressure	totalPressure	fixedFluxPressure	fixedFluxPressure	fixedFluxPressure	symmetryPlane

The method of investigation consisted of changing various parameters of the simulation model, influencing the way a solution is reached, and comparing the CPU time and results.

### 3.4.2 Finite Volume Schemes

The integration and interpolation schemes for the divergence terms of `driftFluxFoam` are shown below. These were kept the same for both models:

```
divSchemes
{
    default           none;

    div(rhoPhi,U)      Gauss linearUpwind grad(U);
    div(tauDm)         Gauss linear;
    "div\(\phi,\alpha.*\)"   Gauss vanLeer;
    "div\(\phi_{irb},\alpha.*\)" Gauss linear;
    div(rhoPhi,k)      Gauss limitedLinear 1;
    div(rhoPhi,epsilon) Gauss limitedLinear 1;

    div(((rho*nuEff)*dev2(T(grad(U))))) Gauss linear;
}
```

These various schemes are briefly explained in section 3.3, except the turbulent terms  $k$  and  $\epsilon$  have the interpolation scheme `limitedLinear` applied. This is a variant of `linear` interpolation, but limited towards `upwind` in cells of high rate of change of gradient. The coefficient of 1 denotes the strongest enforced limiting.

### 3.4.3 Finite Volume Solution

The linear-solver of the pressure field, the role of which was discussed previously in section 3.3, was to be changed, and its affect compared. For the first model, the pressure block in `fvSolutions` was written to be:

```
p_rgh
{
    solver          GAMG;
    tolerance      1e-07;
    relTol         0.01;
    smoother       GaussSeidel;
    cacheAgglomeration true;
    nCellsInCoarsestLevel 20;
    agglomerator   faceAreaPair;
    mergeLevels    1;
}
```

This implements the GAMG matrix inversion scheme with a `GaussSeidel` smoother. To control this multi-grid method the coarsest level was capped at 20 cells, shown in the line `nCellsInCoarsestLevel 20`. This was based on research of other cases, but adjusted to the mesh in use.

This solution scheme was to be compared to a PCG method:

```
p_rgh
{
    solver          PCG;
    preconditioner DIC;
    tolerance      1e-07;
    relTol         0.01;
}
```

Note the tolerances were set to the same, so any impact was due to the linear-solver

itself. All other conditions of the model were kept the same, to maintain a controlled investigation.

With regard to simulation initialisation, the decision was made to run the models on the University of Exeter's CEMPS remote server cluster. For a more rapid solution time, they were run in parallel over 16 cores each. The elapsed CPU time to model 600s will be compared, and quality of results.

Once remotely logged into the respective server, terminal commands to initialise the simulation were as follow::

```
decomposePar  
mpirun -np 16 renumberMesh -parallel  
mpirun -np 16 driftFluxFoam -parallel >log.1 2>&1&
```

This command string split the case across the 16 cores, renumbered the mesh and ran the `driftFluxFoam` application solver in parallel. Outputs were written to a `log` file.

### 3.4.4 Outcome

The findings of this preliminary study were to be used in the case set-up for the Swirl-Flo®, thus, are presented here rather than the formal results section.

Reading the log files of the two finished cases, the run times were found to be:

GAMG:

```
Execution Time = 406766 s    ClockTime = 406947 s
```

PCG:

```
Execution Time = 466646 s    ClockTime = 466812 s
```

It is of little surprise that the multi-grid solver had a shorter CPU time. However, the results of the simulation models themselves had to be compared, to make the faster solving time worth while. The finished cases we reassembled for post-processing using the command:

```
reconstructPar
```

The behaviour of the dispersed phase,  $\alpha$ , was also inspected. Figure 3.2 shows the sludge bed and flow down the underflow for each model.

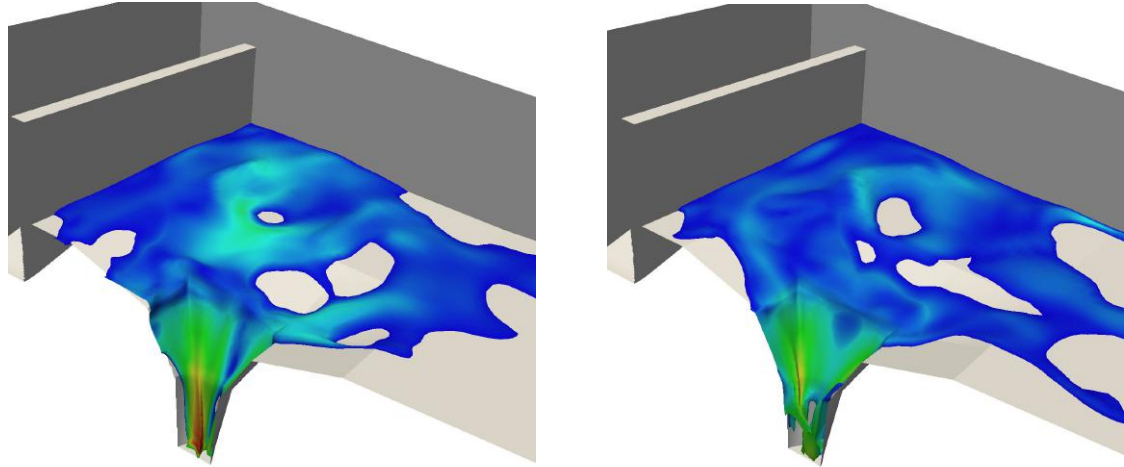


Figure 3.2: Sludge bed formation of GAMG (left) and PCG (right) solutions

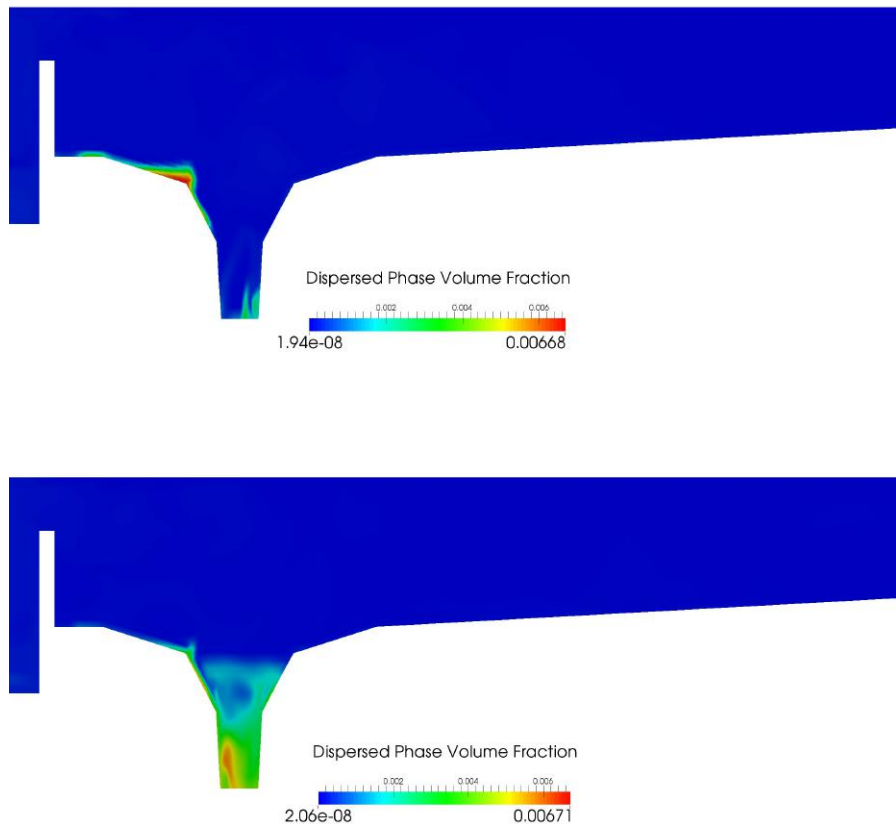
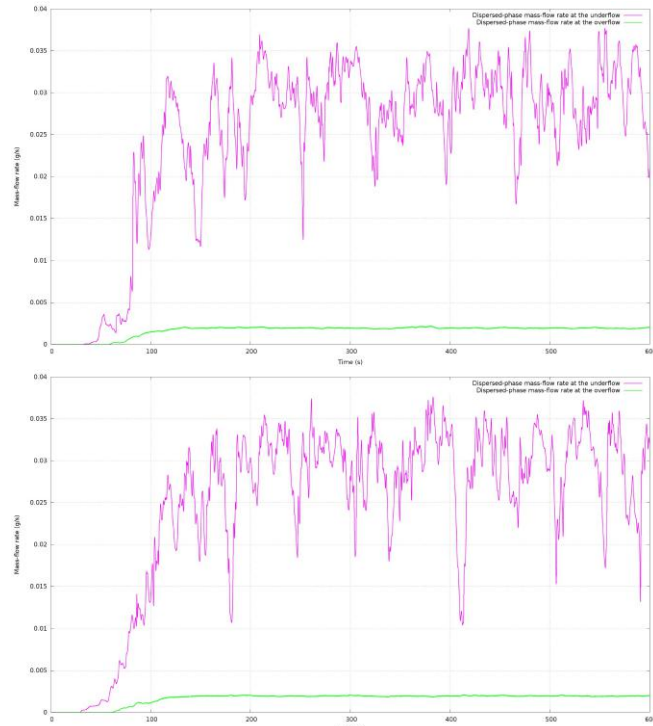


Figure 3.3: Profiles of dispersed phase volume fraction of GAMG (top) and PCG (bottom) solutions

Although rather different on inspection, the shape of the sediment bed is one of limited importance. Little is described about tank performance from studying this, but included nonetheless as an indication to the simulations producing physically applicable results. Furthermore, because of the complex nature of particle settling, it is unlikely the simulation would accurately replicate the laboratory results in this manner. The judgement can be made, however, that both GAMG and PCG models produce a result that is superficially realistic. More quantitative data is needed however.



*Figure 3.4: Mass flow rates of dispersed phase volume fraction of GAMG (top) and PCG (bottom) solutions*

Figure 3.4 shows the dispersed phase mass flow rates at underflow and overflow. Activity at the overflow looks very similar for both solvers, at what could be expected from performance of the RT. After a short delay dispersed phase particles arrive at the overflow, at low mass flow rate, showing separation has occurred. The rather consistent flow rate suggests a steady state has been reached. The underflow, however, displays great variation and erratic changes in flow rate. This could be due to the way dispersed phase enters over the first weir and could immediately flow down the hopper, or settling as a sludge bed. This means it is unlikely a uniform relationship would be displayed, as this is of a more chaotic behaviour. This could be described as a quasi-steady state. Further analysis

of this type of result is discussed in [4]. It is therefore accepted that both models are performing in a stable manner. In the context of this preliminary investigation, it is the differences between the two models that is of greatest concern. After post-processing it is concluded that reliability of the two models is similar, and there would be no advantage to using the longer-running PCG model.

GAMG solver ran 12.8% faster than PCG. This is of little surprise, the literature suggests GAMG to be used for a faster solution, whereas PCG is utilised for stability. Due to negligible stability discrepancy between cases, the resolution of the mesh and time restraints, GAMG was used. Optimum tolerances for the pressure field were found to be: `tolerance = 1e-7, relTol = 0.01`. These conditions were then taken forward for the running of the Swirl-Flo<sup>®</sup> case.

### 3.5 Settling Model Implementation

A further method to ensure relatability between computational and experimental studies was to ensure the correct drift velocity was defined for the Drift Flux Model. This was to accurately represent the physical settling velocity of the sediment used in the laboratory. The associated experimental group of this report were investigating the applicability of using olive stone powder (OSP) as a substitute for primary sludge modelling by physical experiment [2, 18, 26]. In context of mathematical modelling, as layed out in this report, four settling models were formulated from empirical study, [26], the values of which affect the term  $\nu_{dj}$  in the Diffusion equation 21. The differing rheological models were to represent various scenarios of the case two-phase fluid; secondary sludge, half OSP-half sludge and OSP from batch tests. These models were further implemented into the CFD domain as part of this investigation. The rheology of both continuous and dispersed phases are described in `transportProperties`. The viscosity of each model was subject to the `slurry` parameter, and the relative velocity model set as `general`. The coefficients of model 3, OSP batch tests, and how they were implemented are shown below as an example:

```

"(simple|general)Coeffs"
{
    V0          (0 -0.00109 0);
    a           1064.12;
    a1          10813.76;
    residualAlpha  residualAlpha [0 0 0 0 0 0] 1.28295e-5
}

```

These coefficients were changed for four models. The reader is referred to [26] for an in depth account of this approach.

### 3.6 Optimum Case Setup for Swirl-Flo®

The purpose of the preceding studies have been to gain experience and a basis of knowledge to fabricate reliable and stable OpenFOAM® case files, that accurately represent the behaviour of the OSP Swirl-Flo® empirical experiments. Section 3.2 documents the research into multi-phase modelling techniques culminating in the decision to use the Drift Flux Model, utilised in the form of the solver application `driftFluxFoam`. Further theory in section 3.3 illustrates the techniques of controlling the behaviour of the solver in the CFD domain, whereas section 3.4 tests these techniques in practice. The following section describes method of the main objective and deliverable of this project; applying the findings from the aforementioned study to an optimum Swirl-Flo® case.

A mesh of 4,391,672 cells was again provided (see [17, 23]). Table 3.2, below, shows the initial and boundary conditions applied to the model.

*Table 3.2: Initial Conditions for the Swirl-Flo®*

Parameter	Inlet	Overflow	Underflow	Walls	Water Level
U	fixedValue	pressureInletOutletVelocity	fixedValue	fixed Value	slip
alpha.sludge	fixedValue	inletOutlet	zeroGradient	zeroGradient	slip
p_gh	fixedFluxPressure	totalPressure	fixedFluxPressure	fixedFluxPressure	fixedFluxPressure

The same parameters described in section 3.4 for `fvSolutions` and `fvSchemes` were used. The justification of this shall be discussed later, in section 5.

In terms of post-processing, a standardised sampling scheme was devised between experimental and computational sides of the group. This was to ensure comparison of results could be with reference to one another. Tangential velocity profiles at each point shown in figure 3.6 were to be produced and compared, as well as dispersed phase concentration variation as the experiment ran. A `sampleDict` was written, to read values for components of velocity in  $x$   $y$  and  $z$  at the velocity profile measurement points. From this, tangential velocity shall be calculated. Concentration of dispersed phase would be measured at the overflow and underflow. The same origin and frame of reference was used for Baker's [2] related empirical study, and Lowe's [17] Volume of Fluid (VOF) investigation, hence the other points.

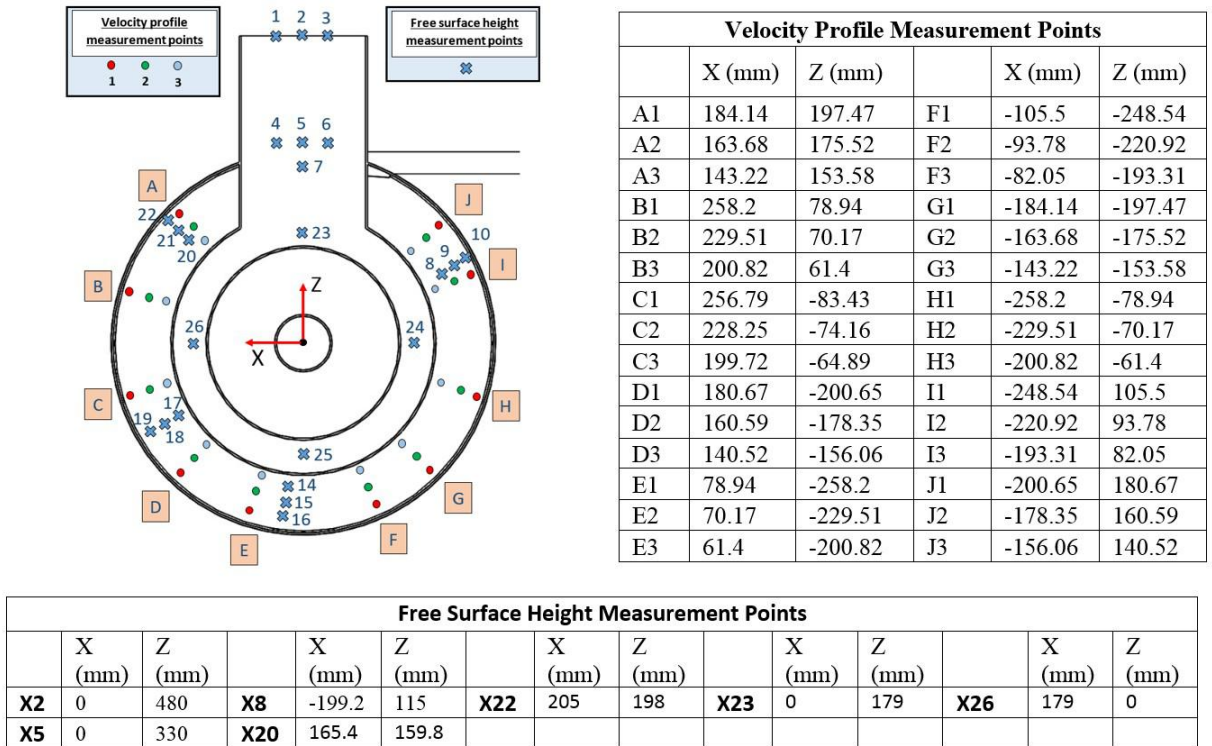


Figure 3.5: Illustration of sample points, retrieved from [17]

Once uploaded to the server, the Swirl-Flo<sup>®</sup> case was split over 24 cores, and initialised in a similar manner to the RT simulations in section 3.4:

```
decomposePar
```

```
mpirun -np 24 renumberMesh -parallel
```

```
mpirun -np 24 driftFluxFoam -parallel >log.swirlFlo 2>&1&
```

## 4 Presentation of analytical results

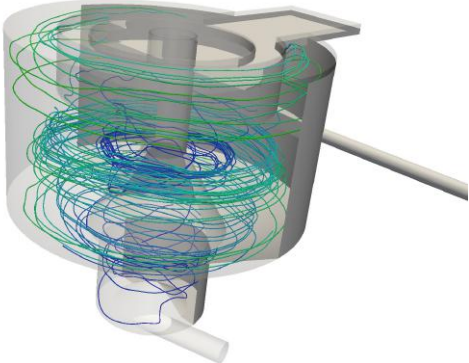


Figure 4.1: Velocity streamlines for Swirl-Flo®

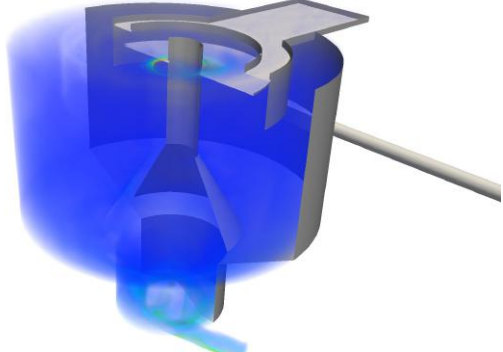


Figure 4.2: Volume plot of dispersed phase,  $\alpha$

Figures 4.1 and 4.2 show velocity streamlines, and volume fraction of dispersed phase  $\alpha$ , throughout the body of the Swirl-Flo® tank. No truly meaningful or quantitative conclusions are intended to be drawn from these figures (hence the lack of a scale). They are included here as an illustration of how the model behaved in a physically ‘realistic’ manner; the dispersed phase has been subject to vorticity, and is responding in such a way. A small sludge bed has formed at the bottom of the tank and the overflow baffle plate. This initial, surface glance of post-processing can just give confirmation of the initial and boundary conditions applied to the case. From this point, more in depth analysis can continue.

The simulation was run for a much shorter time than desired; 133.5 seconds of simulation. The reasons and implications of which will be discussed in section 5.

**Execution Time = 1618160 s**

**Clock Time = 1655478 s**

**Time = 133.5015 s**

As mentioned, the main way computational and empirical results are to be compared is the relation of tangential velocity profiles and concentration plots at the outlets.

## 4.1 Tangential Velocity Profiles

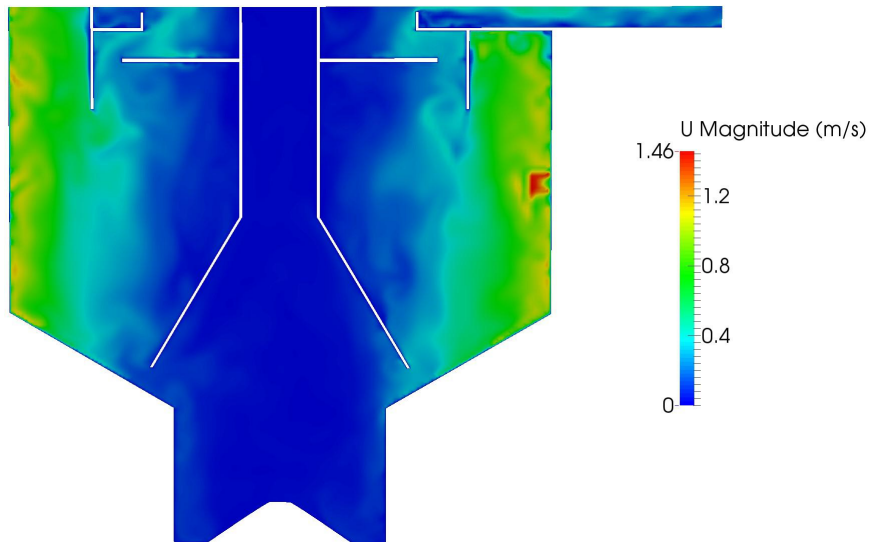


Figure 4.3: Velocity magnitude through the depth and width of Swirl-Flo ®

The velocity distribution of the profile in figure 4.3 further suggests a fluid vortex is present. A higher velocity magnitude around the peripherals of the tank and presence of a small viscous boundary layer, imitate the real fluid flow conditions. The small hot spot of high velocity is where the inlet pipe enters the tank.

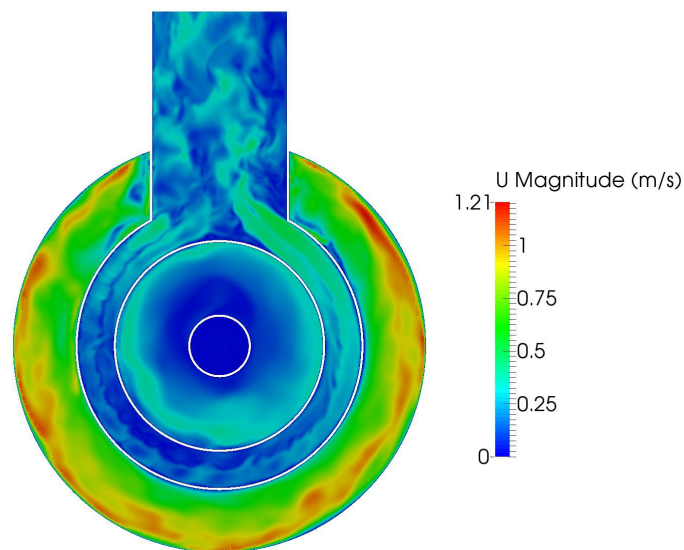
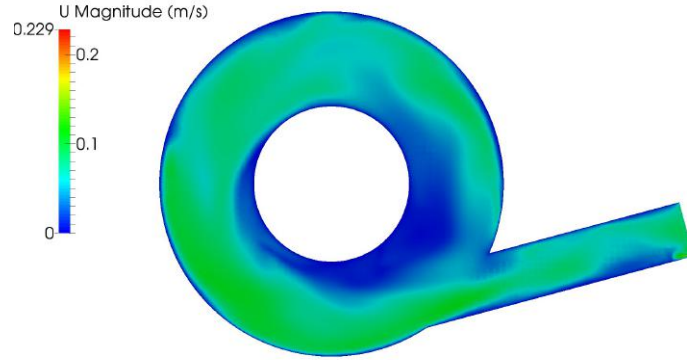


Figure 4.4: Velocity magnitude across the overflow

High velocity around the edges of the tank, in figure 4.4, further support swirling motion. Fluid is also exiting the tank at the overflow, at a lower velocity. The fluid behaviour at the overflow tray is realistic, but erratic, suggesting steady-state has not been reached and transient conditions are still present in the tank.



*Figure 4.5: Velocity magnitude across the underflow*

The low velocity at the underflow, shown in figure 4.5, are as expected. This zone is where the settled dispersed phase exits the tank as a sludge bed, and should do under a low flow.

Figures 4.3, 4.4 and 4.5 show the variation of velocity throughout different areas of the tank. The higher velocity magnitude around the edge suggest phase separation is occurring, due to the flow vorticity (section 1.2.2). For quantitative data that is truly relatable to the empirical study, tangential velocity was calculated from sampled velocity components.

There were two experimental methods to record tangential velocity at the sample points, performed by Baker [2]. The results from a propeller-meter and of an acoustic doppler were plotted against simulation velocity profiles. In the interest of brevity, tangential velocity profiles of only five measurement points will be presented here. Plots at every sample point are available upon request.

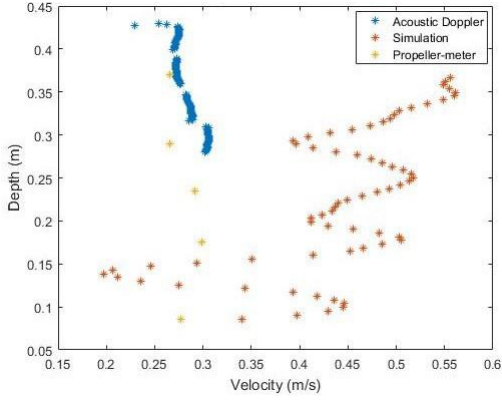


Figure 4.6.1: Velocity profiles at point A2

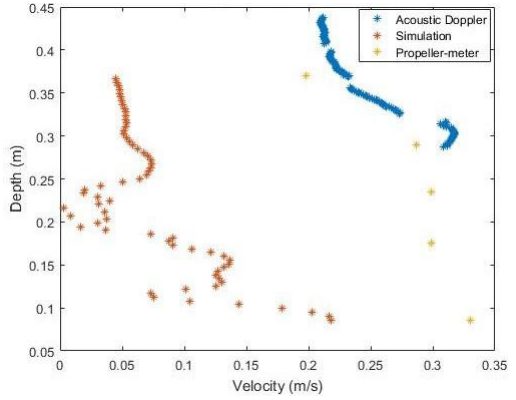


Figure 4.6.2: Velocity profiles at point C2

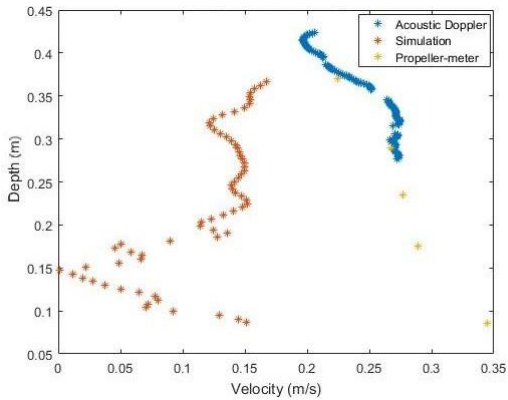


Figure 4.6.3: Velocity profiles at point D2

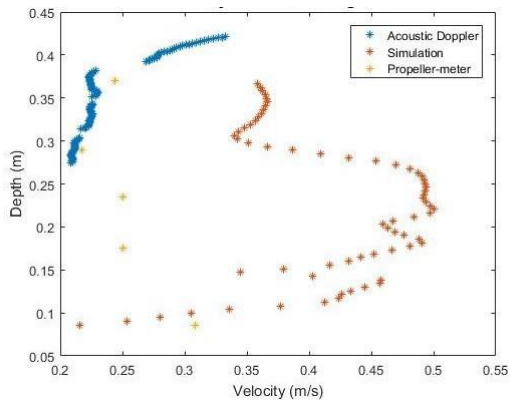


Figure 4.6.4: Velocity profiles at point F2

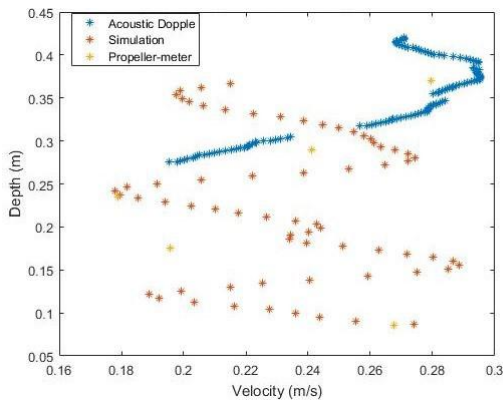
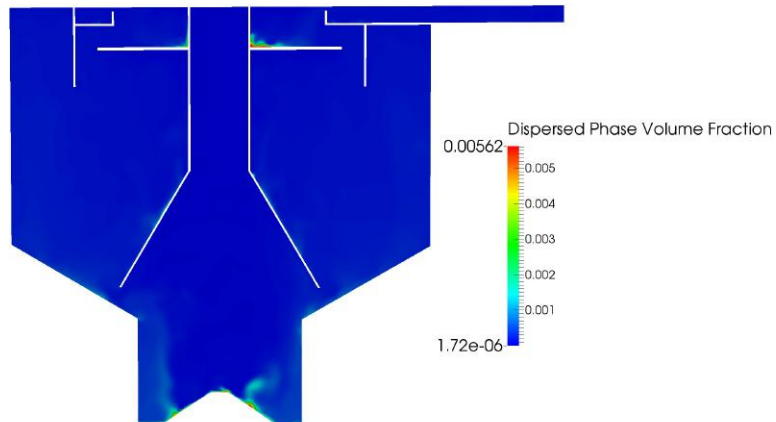


Figure 4.6.5: Velocity profiles at point I2

The velocity profiles seen in figures 4.6.1 - 4.6.5 compare simulation and two different methods of empirical study. The difference in simulation and empirical results are relatively large. The acoustic doppler and propeller-meter results are similar to each other, so there is validation in the experimental regard [2], however the discrepancy in CFD results could be due to short run time. With this said, the simulation and experimental

results follow a similar form. Although the specific values of velocity are different, it can be seen that there is a trend. One could speculate that perhaps, if the simulation had been run for longer, the results would be more similar.

## 4.2 Volume fraction of Dispersed Phase



*Figure 4.7: Volume Fraction of Dispersed Phase through the depth and width of Swirl-Flo<sup>®</sup>*

The graphical profile in figure 4.7 shows the areas where OSP has settled, or is still dispersed. The main sludge beds are seen at the underflow and settling on the upper baffle plate. This behaviour is an accurate representation of the performance of the physical Swirl-Flo<sup>®</sup>. This can show that the virtual tank is working properly as a primary settling tank. Closer inspection of the sludge beds can give more detailed information of the tank behaviour.

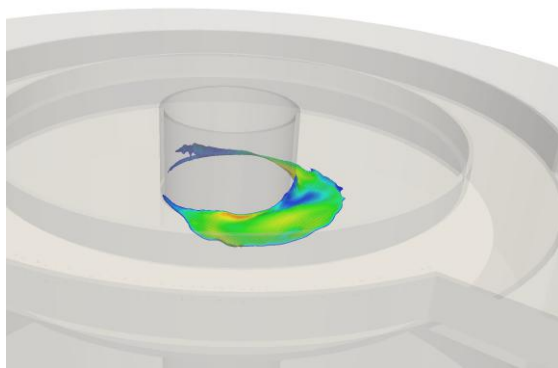


*Figure 4.8: Velocity streamlines for Swirl-Flo<sup>®</sup>*

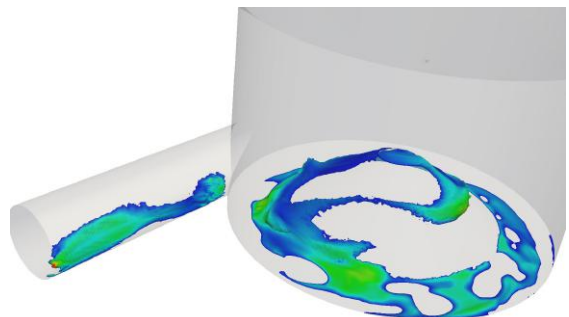


*Figure 4.9: Volume plot of dispersed phase,  $\alpha$*

Figures 4.8 and 4.9 show the majority of OSP settling down to the underflow, and sludge leaving through the underflow. This is the main procedure of settling in HDVS's of this type, and can therefore show some comparability to empirical study on a superficial level. There is also a small catchment towards the upper geometry of the tank. This suggests a small volume of OSP may be leaving the overflow as well. Predicted by the associated experiments, the tank is not expected to be 100% efficient as primary settling tanks are one in a series of water treatment devices, mentioned in the background to this project. Similar to the velocity profiles, plots of dispersed phase concentration at the overflow and underflow were compared between empirical and computational results.

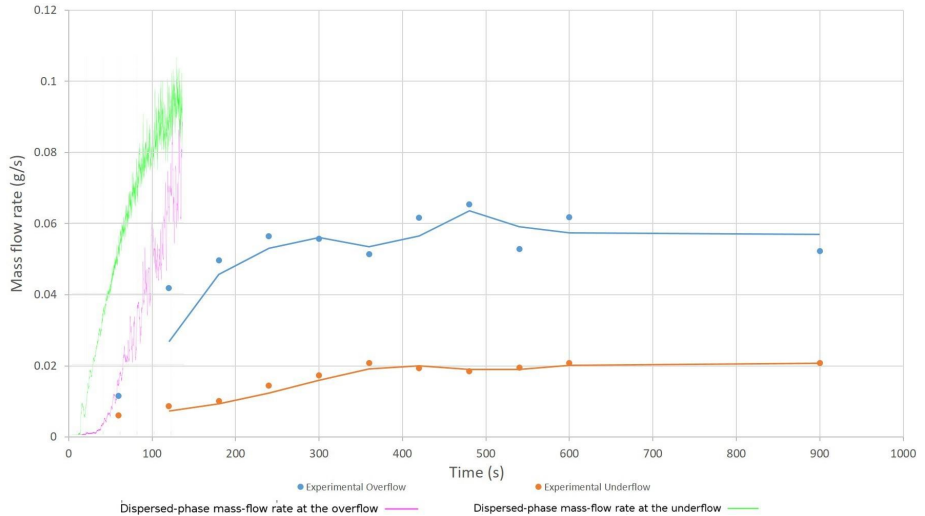


Figure 4.10: Comparison of dispersed phase concentration at both outlets, produced by [2]

Figure 4.10 further confirms that the reduced simulation time has a profound affect on the reliability of results, and reduces ability to make meaningful conclusions from comparison to empirical data.

## 5 Discussion and Conclusions

The preceding sections document the study and research of the Drift Flux Model of multiphase flow, its implementation into OpenFOAM® and subsequent fabrication of HDVS simulation case files. The velocity profiles of section 4.1 seem to follow a similar trend to the experimental results, yet hold differing specific values. A similar disparity is

seen in the analysis of dispersed phase concentration, seen in section 4.2.

Differences of this magnitude mean that, at this point, the CFD model cannot be validated from empirical data.

The predominant cause of this was the short time the Swirl-Flo® simulation was run for; more simulation time would allow any transient behaviour to dissipate, and more reliable conclusions to be drawn. Under estimation in the solution time of the solver application `driftFluxFoam` was a large contributor to the reduction of CPU time. It took 19 days to calculate 133 seconds, meaning an advisable 5 minutes of simulation time would require 43 days. Such a timescale is beyond the scope of this project. Another hindrance of simulation time was the repetitive crashing of the server cluster. Thus, the culmination of long solution time and recurring server faults meant that an insufficient time-scale was the fundamental cause of setbacks in this project, and therefore disparity in results.

Although direct comparison was not possible, attempted validation of the model came in the form of speculative assessment; essentially extrapolating the results based on the available Swirl-Flo® case simulation. The simulation behaved in a desired and expected manner, suggesting that the study into providing optimum case files was a success. Results may be more similar to the empirical case if steady state could be reached. With this said, the preliminary studies of section 3.4 were performed on a different geometry and mesh. The Swirl-Flo® case, therefore may not have been fully optimised. A larger timescale for this project could have allowed for preliminary runs using the same mesh as the main case, to ensure the most efficient run. However, the conclusion can be drawn that the case files are those of a high grade HDVS CFD simulation, within the context of this project.

Suggested future work from this project would be to further optimise the running of the Swirl-Flo® case. As detailed above, an extensive execution time can be planned and accounted for leading to a steady-state solution. The modelling of turbulence would also be advised, to increase accuracy to the empirical case. The subject of turbulence modelling was omitted in this project, to not exacerbate an already lengthy execution. The added computational effort of a turbulent multi-phase flow would lead to mere seconds of resolved simulation time upon conclusion of this investigation.

## **6 Project management, consideration of sustainability and health and safety**

The project success was impacted greatly by technical difficulties and miss-alignment of timescale. The work package taken on was unachievable to the satisfaction of the author in the time frame. As previously discussed, under estimation of execution time to run a simulation using the `driftFluxFoam` application solver was highly influential. Extensive research went into the selection of a multi-phase model at the beginning of the assignment. The selected Drift Flux Model is a simplification, used by many others in previous studies. The extensive solution time was therefore unexpected. Earlier consideration of this factor may have improved results, however essential preliminary work can only leave a finite time for simulation within the project time frame. The reviewed literature makes little mention of computational resources used, a point this project aims to rectify.

Progress was further hindered by the repetitive down-time of the cloud server service, costing multiple days worth of available solution at a time. The scale of these difficulties could not be foreseen in the initial project management phase. Although initial work flow planning accounted for technical difficulties, disruptions of this extent were highly improbable. If full project closure is required the simulation can be re-initialised on the University of Exeter's CEMPS servers, for hope of improved data post-deadline.

The servers used in this project are a utility available for anyone with the correct permissions. Consideration of other users had to be taken into account; running over too many cores and for too long would impede others' investigations. Use of the servers was conducted in a professional manner and with respect for other projects.

As this investigation was of a computational nature, there was little cause for concern over health and safety or sustainability. In fact, one of the main draws of the field of CFD is the prospect of sustainability. Computational simulation offers an alternative to resource intensive laboratory experiments, rendering the energy consumption negligible by comparison.

## 7 Contribution to group functioning

This individual investigation contributes to an overall group effort [3]. For a smooth collaborative process to be achieved, clear and professional communication had to be present between the seven authors.

Success in this report depended upon receiving work and results from others, and *vica versa*. For a CFD model to be fabricated, a mesh must be produced. These were all produced by Lowe and Scobell [17, 23]. The performance of early mesh iterations had to be relayed back to the meshing team, to meaningfully further the mesh design cycle. This process was essential as a setback in one project path may impede another, delaying the overall project deliverable.

A key objective of this investigation was to produce a CFD model representative of the physical model. For this to be achieved, settling models from Wye [26] were implemented. Those simulations were subsequently run and results handed back, providing a useful asset in the investigation into OSP. The equivalent empirical study into velocity and separation behaviour of the Swirl-Flo® was performed by Baker [2]. Comparison and validation of respective outcomes required mutual assessment of results, and a collaborative conclusion.

As the main creator of the Swirl-Flo® case files, the author contributed to the mutual group aim by providing the computational model for a HDVS. This was used in conjunction with the related empirical study, to achieve the group aim of investigating the use of OSP as a substitute for primary sludge modelling. Findings from preliminary research and simulation studies were utilised to produce as reliable and high grade product as possible.

The overall accomplishment of the group can be attributed to a strong focus on communication and support between members. Throughout the project, timely achievement of individual objectives and sharing of information culminated in a successful group effort.

## 8 References

- [1] Ahern, D. (2017) "Study and Improvement of the Performance of an Industrial Settling Tank using CFD Models in OpenFOAM®" Universitat Politècnica de Valéncia
- [2] Baker, A. (2018) "Validation of Sedimentation Tanks through Empirical Studies", MEng I2 Project - University of Exeter
- [3] Baker, A. Bentley, R. Lowe, J. Mendoza, M. Russell, T. Scobell, T. Wye, A. "Experimental and Numerical Investigation into the Use of Olive Stone Powder as a Substitute for Primary Sludge Modelling", MEng G2 Project - University of Exeter
- [4] Bentley, R. (2018) "An Investigation into MULES and its Application into Simulating Settling Behaviour in an Armfield Rectangular Settling Tank", MEng I2 Project - University of Exeter
- [5] Brennan, D. (2001) "The Numerical Simulation of Two-Phase Flows in Settling Tanks", Imperial College of Science, Technology and Medicine
- [6] Burt, D. (2010) "Improved Design of Settling Tanks Using an Extended Drift Flux Model", MMI Engineering
- [7] Dahl, C. (1993) "Numerical Modelling of Flow and Settling in Secondary Settling Tanks", Dept. of Civil Engineering, Aalborg University
- [8] Elghobashi, S. (1994) "On Predicting Particle-laden Turbulent Flows", Applied Scientific Research
- [9] Gisiotti, D. (2006) "The Rankine Vortex Model", Regional Meteorological Observatory
- [10] Ishii, M. and Hibiki, T. (2011) "Thermo-fluid Dynamics of Two-Phase Flow" 2nd. ed, Eyrolles, Springer
- [11] Jarman, D. (2011) "A study of the Design of Cylindrical Vortex Flow Controls for Use in Urban Drainage Systems", PhD Thesis - University of Exeter
- [12] Jarman, D. (2016) "An introduction to vortex flows and their implications on solid-liquid separation" Hydro International [online], available at: [www.advancedgritmanagement.com](http://www.advancedgritmanagement.com) [accessed 3rd Apr. 2018]
- [13] Kallio, S and Akademi, A (1996) "On the Mixture Model for Multiphase Flow", Valtion teknillinen tutkimuskeskus (VTT)
- [14] Larsen, P. (1977) "On the Hydraulics of Rectangular Settling Basins - Experimental and Theoretical Studies", Dept. of Water Resources Engineering, Lund, Sweden
- [15] Lee, J.H. Bang, K.W. Choi, C.S. Lim, H.S. (2010) "CFD modelling of Flow Field and Particle Tracking in a Hydrodynamic Stormwater Separator" Water science and technology: a journal of the International Association on Water Pollution Research
- [16] Liu, X. and Garcia, H. (2011) "Computational Fluid Dynamics Modeling for the Design of Large Primary Settling Tanks", Journal of Hydraulic Engineering
- [17] Lowe, J. (2018) "Investigation into Mesh Generation using snappyHexMesh for a Model Sedimentation Tank and Hydrodynamic Vortex Flow Separator including Volume of Fluid Simulations", MEng I2 Project - University of Exeter
- [18] Mendoza, M. (2018) "Determination of a Viscosity Model for an Olive Stone Poweder and Water Suspension for Primary Sedimentation Tank Modelling", MEng I2 Project - University of Exeter

- [19] Nelson, M. (2015) “OpenFOAM® in Wastewater Applications: 4 - Simulation Process” [Tutorial Slides] bluecaPe, Available at: rsamstag.files.wordpress.com
- [20] Openfoam.com (2018) Source files Available at: OpenFOAM®: *applications/solvers/multiphase/driftFluxFoam/driftFluxFoam.C*, [online] Accessed 3rd April 2018
- [21] Sansalone, J. and Pathapati, S. (2009) “Particle Dynamics in a Hydrodynamic Separator Subject to Transient Rainfall-runoff” Water Resources Research
- [22] Schmitt, V. Dufresne, M. Vazquez, J. Fischer, M. Morin, A. (2013) “Separation Efficiency of a Hydrodynamic Separator Using a 3D CFD Approach” Ecole Nationale du Génie de l’Eau et de l’Environnement de Strasbourg
- [23] Scobell, T. (2018) “Investigation into Mesh Generation Techniques Using Pointwise® on Primary Sewage Sedimentation Devices” MEng I2 Project - University of Exeter
- [24] Stamou, A. and Rodi, W. (1989) “Numerical Modeling of Flow and settling in Primary Rectangular Clarifiers” Journal of Hydraulic Research
- [25] Tabor, G. (2017) “Introduction to OpenFOAM® Lecture 4. Numerical Aspects of CFD” ECMM148: Computational Modelling Lecture series - University of Exeter
- [26] Wye, A. (2018) “Investigation and Development of a Mathematical Model to Describe the Settling Characteristics of Olive Stone Powder” MEng I2 Project - University of Exeter

